Available online at www.sciencedirect.com

SCIENCE DIRECT®

Earth and Planetary Science Letters 228 (2004) 177–194

EPSL

www.elsevier.com/locate/epsl

ENSO and Indian Ocean subtropical dipole variability is recorded in a coral record off southwest Madagascar for the period 1659 to 1995

J. Zinke*, W.-Chr. Dullo, G.A. Heiss, A. Eisenhauer

Leibniz Institute für Meereswisenschaften, IFM-GEOMAR, Wischhofstrasse 1-3, 24148 Kiel, Germany

Received 22 September 2003; received in revised form 2 September 2004; accepted 22 September 2004
Editor: E. Bard

Abstract

The Ifaty coral record from off SW Madagascar provide a 336-year coral oxygen isotope record that is used to investigate the natural variability of the western Indian Ocean subtropical SST dipole and ENSO. The coral oxygen isotope record primarily reflects past sea-surface temperature (SST) variability on seasonal to multidecadal scales. To validate the SST reconstructions derived from oxygen isotopes, Sr/Ca ratios were obtained for selected time windows (1973–1995, 1863–1910, 1784–1809, 1688–1710). The period 1675–1760 was found to be the coolest period of the entire record with anomalies of 0.3–0.5 °C that includes the Late Maunder Minimum (1675–1710). The warmest periods, as indicated by our data, occur between 1880 and 1900 and the upper part of the Ifaty record (1973–1995).

We generated a time series of coral $\delta^{18}O$ for different seasons of the year to investigate austral winter and summer SST variability that influences rainfall intensity over southern Africa. Winter coral $\delta^{18}O$ is coherent with winter SST on decadal and multidecadal time scales between 1854 and 1995. We suggest that the Ifaty winter time series provides a record of winter SST variability over the Mozambique Channel/Agulhas Current region over 336 years.

Strong Indian Ocean subtropical dipole events, occurring during austral summer, are displayed in the Ifaty record. The austral summer coral $\delta^{18}O$ is coherent and in phase with ENSO indices on interannual time scales (2–4 years) between 1880–1920, 1930–1940 and after 1970. Our data indicate that the impact of ENSO on SW Indian Ocean SST and atmospheric circulation was also strong between 1680–1720 and 1760–1790, in agreement with other studies. We show evidence that these variations are caused by changes in the regional hydrologic balance. The results demonstrate that the impact of ENSO cycles in the region of the SW Indian Ocean has changed significantly since 1970 and relate to a warming of southwestern Indian Ocean surface waters altering the spatial signature of ENSO.

Keywords: corals; oxygen isotopes; trace elements; paleoclimatology; Indian Ocean subtropical dipole events; ENSO

* Corresponding author. Present address: Vrije Universiteit Amsterdam, De Boelelaan 1085, 1081 HV Amsterdam, Netherlands. Tel.: +31 204447327; fax: +31 206462457.
E-mail address: zinj@geo.vu.nl (J. Zinke).

0012-821X
doi:10.1016/j.epsl.2004.09.028

1. Introduction

Geochemical parameters in skeletons of massive corals have been used to infer past changes in climate on interannual to multidecadal time scales, e.g. sea-surface temperature (SST), salinity (SSS), upwelling intensity, river runoff and oceanic advection [1–8]. The oxygen isotope composition is the most widely used geochemical fingerprint in coral palaeoclimatology. In regions with a constant hydrological balance it predominantly provides SST variations. In regions with variations in the evaporation–precipitation balance (E–P), and/or oceanic advection, it provides variations in the isotopic composition of seawater ($\delta^{18}O_{seawater}$). Ultimately, SSS may be recontructed [1,7,8]. The potentially long life time of decades to centuries and growth rates between 1 and 2 cm per year in corals provides high-resolution geochemical records for several centuries that allow study of natural climate variability under different boundary conditions, e.g. the so-called Little Ice Age (LIA; 1400–1900) [9–11].

Previous work has indicated the importance of SST anomalies in the Mozambique Channel and Agulhas Current region in controlling rainfall variability over South Africa and its close relationship to interannual ENSO events [12–24]. Interdecadal variability in the southwestern Indian Ocean was shown to arise through a combination of basin-scale atmosphere–ocean interaction and remote forcing by the Indonesian throughflow and the South Equatorial Current [16,18,25]. South African decadal rainfall variability was linked to 'ENSO-like' decadal variability in SST and atmospheric circulation patterns [26,27]. These changes in background climate may strenghten or weaken the local impact of seasonal to interannual climate phenomena, i.e. ENSO events.

Recent studies have indicated that SST anomalies in the subtropical southern Indian Ocean show interannual dipole events (SIOD), which are phase-locked to the austral summer season [28–30]. Variations in the strength of the southern subtropical high lead to a cooling in the eastern subtropical Indian Ocean off Australia via evaporation and vertical ocean mixing and to warming in the southwestern Indian Ocean south of Madagascar via reduced evaporation. A positive southern dipole results in intensification of rainfall over many regions in Southern Africa that have large socio-economic impact. Comparison of the southern dipole with ENSO and the tropical dipole revealed that it is independent.

Recently, the importance of austral summer subtropical Indian Ocean SST anomalies in controlling the strength of the Indian Monsoon was documented over the short term [31]. Longer palaeoclimatic records are required to assess the occurrence of such dipoles through time. Instrumental records of climate variability from the SW Indian Ocean are scarce and often too short to allow evaluation of the extent to which ENSO or internal Indian Ocean phenomena modulate interannual to interdecadal SST variability.

In this study, we present a bimonthly 336 years coral $\delta^{18}O$ record, complemented by Sr/Ca ratios for several time windows, of a *Porites lobata* from the lagoon of Ifaty off SW Madagascar in order to provide a record for the reconstruction of past surface ocean variability. We compare seasonal and interannual variability of our coral oxygen isotope and Sr/Ca record with instrumental records of SST and rainfall. We establish the relation of coral $\delta^{18}O$ to subtropical SST dipole events and the ENSO teleconnections through time.

2. Oceanic and climatic setting

The study site off southwest Madagascar in the Mozambique Channel is part of the western limb of the anticyclonic tropical/subtropical circulation of the south Indian Ocean. Previous work indicates that there is a continuous southward flow of water through the Mozambique Channel [32–35]. Much of the water originates from the Northern tropical Indian Ocean, but data also show a contribution of South Equatorial Current (SEC) waters that round the northern tip of Madagascar (Fig. 1). The flow through the Mozambique Channel (MC) is dominated by a train of large anticyclonic eddies that propagate southward and connect the SEC to the Agulhas Current (hereafter AC) [36,37]. Thus, the flow through the Mozambique Channel contributes significantly to the warm surface flow of the global surface ocean circulation. In the Southern Mozambique Channel (SMCH), waters from the East Madagascar Current (EMC) fed by the southern limb of the SEC appear to round the southern tip of Madagascar [32]. In austral winter, EMC waters

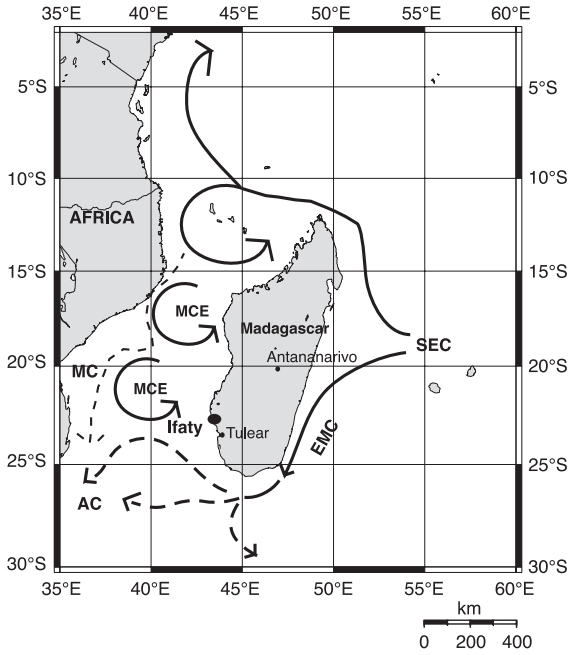

Fig. 1. Map of the southwestern Indian Ocean with the location of the coral core within the lagoon of Ifaty off southwest Madagascar (marked by a black dot). The dominant ocean currents are indicated by lines and arrows [35,36]. SEC=South Equatorial Current, EMC=East Madagascar Current, MC=Mozambique Current, MCE=Mozambique Channel Eddies, AC=Agulhas Current.

appear to cross the SMCH towards the African coast, but often tend to loop up along the west coast of Madagascar [34,35]. The SE trade winds that prevail throughout the year are stronger during austral winter (the SW monsoon season) and lead to an intensified SEC which results in a stronger MC flow [35]. During austral summer the MC flow is at its weakest. Flow through the MC is affected by remote forcing via the strength of the Indonesian throughflow and large-scale wind field variability in the Indo-Pacific region [18,25,38,39].

A 1°×1° gridded seasonal climatology for the study region shows a mean amplitude of the seasonal SST cycle of 5.3 °C over a period of 50 years (Fig. 2) [40,41]. SST in the lagoon of Ifaty has been recorded in situ over 10 months from 1992–1993. Maximum SST's occur during December–March (austral summer) and reach 28.4 °C. Minimum SST's are observed during June–August (austral winter) and reach 21.3 °C. Salinity ranges between 34.9‰ and 35.3‰ [40]. Daily rainfall data show maxima of 130 mm/day between November and February [40]. During June–August precipitation reaches a minimum of less than 25 mm/day. Additional in situ SST and SSS data were recorded for the years 1963–1965 and 1992–1995 in the lagoon of Tulear, which is located about 20 km to the south of our sampling site. Both data sets agree well with gridded SST observations (r^2=0.91). Salinity data between 1963 and 1965 show a larger range than mean climatology, with values ranging between 34.2‰ (February 1964, January 1965) and 35.5‰ (June/July 1964).

The lagoon of Ifaty has a maximum water depth of 11–12 m and is separated from the open ocean by a barrier reef. The continuous swell over the reef top, as well as strong tidal currents (typical tide of 2 m amplitude) through large passages, allow for a good water exchange between the open ocean and the lagoon. The lagoon of Ifaty has no freshwater input from rivers. The Ifaty lagoon lacks input of coastal upwelling because the flat bathymetry offshore inhibits upwelling of colder water masses.

The coral colony studied is situated in the lagoon of Ifaty close to a large passage (Passe d'Ifaty Marohazo) through the barrier reef of Ifaty bay (43°34′ 98″ E, 23°08′ 58 S). The identification of this colony as *P. lobata* is based on methods described by [42]. The colony has grown to a height of about 4.5 m, with a maximum of approximately 5.5 m in diameter. At the sampling date the top of the colony reached the sea surface at low tide and is occasionally exposed. This has led to partial mortality (necrosis) of the central part of the colony surface. At high tide the colony grows at 1.1 m water depth.

3. Materials and methods

The coral core was drilled in October 1995 from a *P. lobata* colony, using a commercially available pneumatic drill. A 406-cm-long core, 36 mm in diameter, was drilled vertically along the growth axis. All cores were sectioned to a thickness of 3 mm and slabs were cleaned in 10% hydrogen peroxide for 48 h to remove organic matter. Then, slabs were rinsed several times with demineralized water and dried with compressed air. For complete removal of any moisture within the coral skeleton the sample was put into an

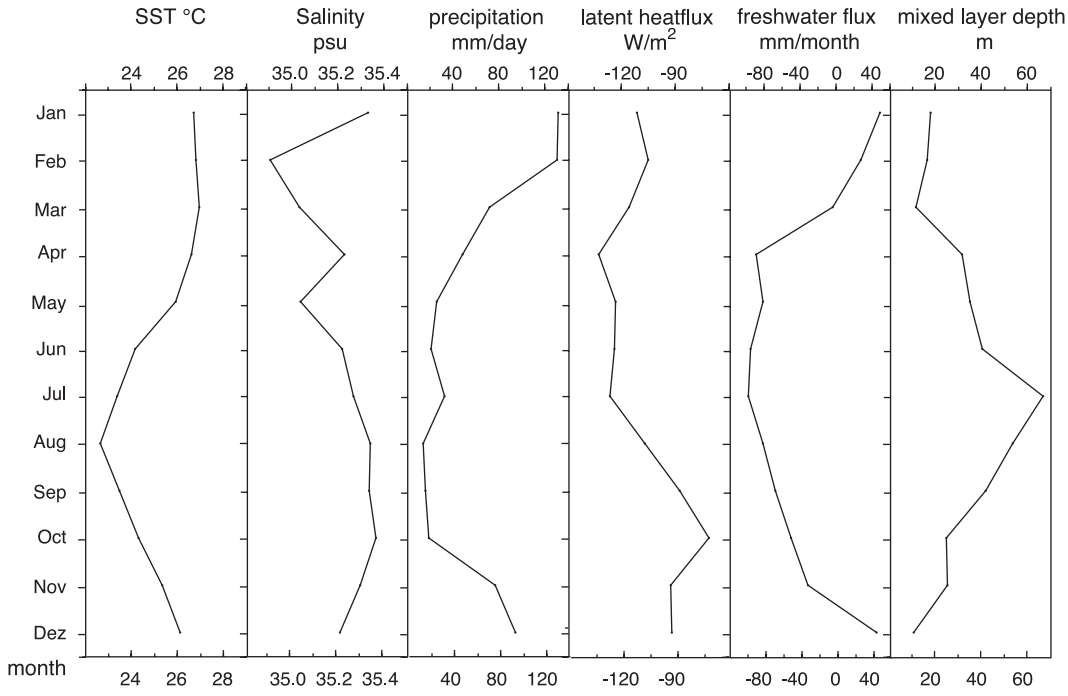

Fig. 2. Monthly climatology of environmental parameters in the relevant grid-box including the Ifaty coral site. Sea-surface temperature (SST), salinity, precipitation, latent heat flux, freshwater flux and mixed layer depth [40].

oven for 24 h at 40 °C. The slabs were X-rayed to reveal annual density banding and to develop a first chronology [43,44] (Fig. 3).

A high resolution profile for stable isotope analysis was drilled using a computer-controlled drilling device along the growth axis as observed in X-ray-radiograph-positive prints to avoid sampling artefacts. Subsamples were drilled at a distance of 1 mm for the years 1995–1920 and 2 mm for the older part of the core; the drilling depth was 3 mm using a 0.5 mm dental drill at 1000 rpm. The growth rate of the coral averages 10 mm/year and our 1 or 2 mm sample spacing provides approximately monthly or bimonthly resolution, respectively.

The samples were reacted with 100% H_3PO_4 at 75 °C in an automated carbonate reaction device (Kiel Device) connected to a Finnigan MAT 252 mass spectrometer (University Erlangen). Average precision based on duplicate sample analysis and on multiple analysis of NBS 19 is $\pm 0.07‰$ for $\delta^{18}O$ (1σ).

Sr/Ca ratios were measured with an inductively coupled plasma atomic emission spectrometer (ICP-AES), which simultaneously collected the respective elemental emission signals. Measurements were carried out at the Institute für Chemie and Biologie des Meeres at the University of Oldenburg (ICBM). We used the technique reported in [45]. Instrumental precision was typically better than $\pm 0.15\%$ relative standard deviation (RSD) for Ca and $\pm 0.08\%$ RSD for Sr (2σ). For the Sr/Ca ratios the error was better than $\pm 0.2\%$ RSD (2σ). The reproducibility of the Sr/Ca ratios of replicate measurements performed on different days was $\pm 0.35\%$ RSD or 0.005 mmol/mol (2σ).

We use the pronounced seasonal cycle in $\delta^{18}O$ and Sr/Ca to develop the final chronology of the coral core and assigned the highest $\delta^{18}O$ and Sr/Ca values to august 15 of each year, which is on average the coldest month. The exact timing of the coldest month varies by about 1–2 months between the years. Thus this approach creates a time-scale error of about 1–2 months in any given year. The $\delta^{18}O$ and Sr/Ca time series were interpolated linearly into 6 and 12 equidistant points for any given year between these anchor points using the Analyseries software [46]. The monthly interpolation was used for a comparison with monthly resolved instrumental data. A bimonthly

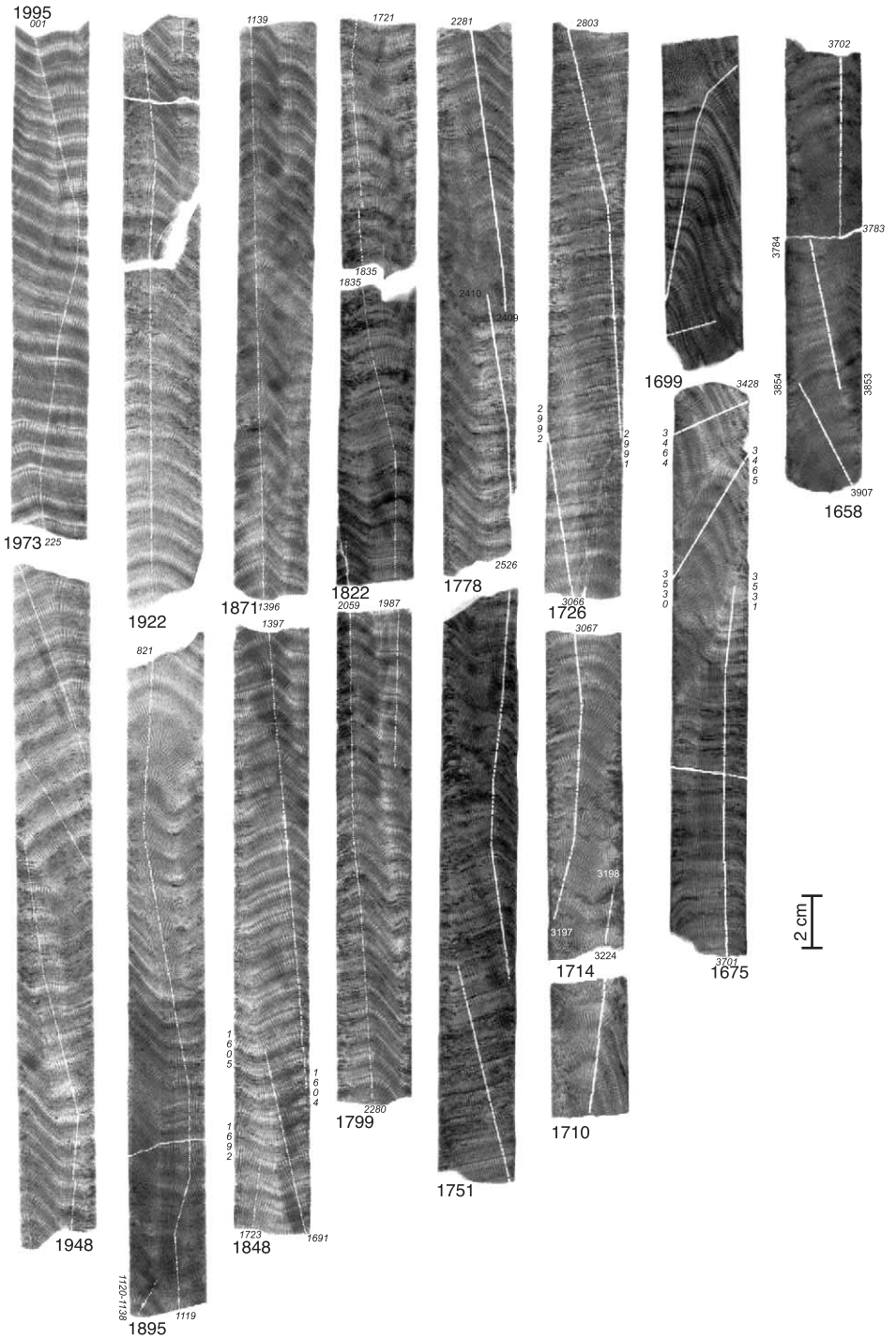

Fig. 3. X-radiograph of coral core Ifaty-4 (*P. lobata*). The white line indicates the sampling transects. The corresponding years are indicated at the top and bottom of each core segment. Note that several overlapping transects were sampled to ensure reproducibility.

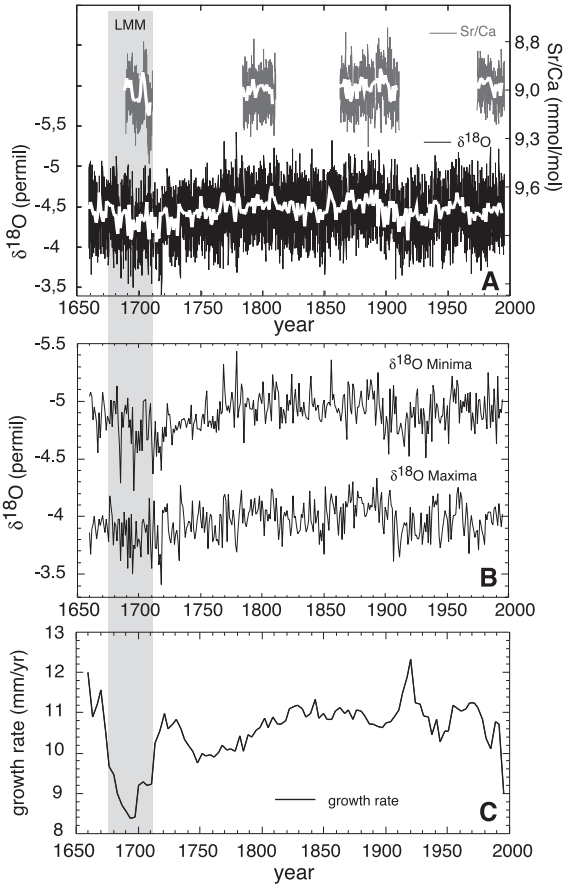

Fig. 4. (A) Ifaty-4 coral Sr/Ca (top) and δ^{18}O (bottom) bimonthly time series with annual means superimposed (solid white line), (B) coral δ^{18}O minima (January/February) and maxima (July/August), (C) annual coral growth rate calculated between the coral δ^{18}O maxima. The Late Maunder Minimum (LMM) is indicated by a shaded vertical bar.

interpolation of the δ^{18}O record was calculated to ensure that sampling resolution does not significantly affect the signals. The bimonthly resolution was used to generate time series of coral δ^{18}O for different seasons of the year (January/February (JF), March/April (MA), May/June (MJ), July/August (JA), September/October (SO), November/December (ND) over the entire record.

SST data were extracted from 1°×1° gridded GISST 2.3 databases (centered at 43.5°E, 22.5°S) for monthly mean temperatures dating back to 1871 held by the Hadley Center for Climate Prediction and Research, UK Metereological Office [47], 2°×2° gridded ERSST v.2 dating back to 1854 [48], and 5°×5° gridded Kaplan-SST global analysis of monthly sea-surface temperature anomalies (SSTA) (centered at 42.5°E, 22.5°S) dating back to 1856 [49].

4. Results

4.1. Long-term trend and growth rate variations

Over the full 336 years of record, the δ^{18}O displays marked positive and negative shifts during certain time periods (Fig. 4). The most positive excursion occurs between 1675 and 1760, including the Late Maunder Minimum of solar forcing between 1675 and 1710 [10]. Further positive δ^{18}O excursions are observed in the mid-19th century (1825–1850), the early 20th century (1900–1938) and the late 20th century (1967–1981) (Fig. 4A). The mid 17th (1650–1675), the late 18th (1750–1800), most parts of the 19th and two periods in the 20th century (1938–1967 and 1981–present) show relative negative δ^{18}O values (Fig. 4A). A multidecadal trend (85–100 years) is evident in coral δ^{18}O throughout the record during all seasons of the year. However,

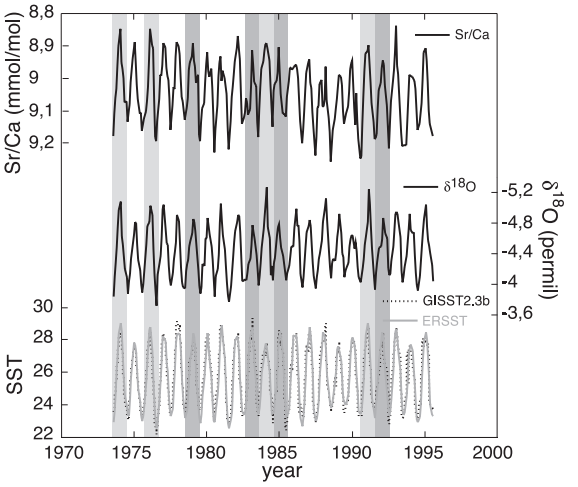

Fig. 5. Monthly variations in Ifaty-4 coral Sr/Ca (top), coral δ^{18}O (middle) and instrumental SST (dashed line=GISST2.3b [47]; solid gray line=ERSST v.2 [48]). The δ^{18}O and Sr/Ca ratios have been interpolated to 12 points per year to allow calculation of correlation statistics with instrumental SST. Wet (light gray) and dry (dark gray) years in the study region, based on precipitation anomalies derived from [57] are indicated by shaded vertical bars.

it is more pronounced during the southern hemisphere summer (November–February) and fall seasons (March–June) (S1).

Sr/Ca ratios were measured for selected time windows at monthly (1688–1710, 1891–1910, 1973–1995) and bimonthly resolution (1784–1809, 1863–1890) (Fig. 4A). The Sr/Ca ratios are lowest for the upper part of the record (1973–1995) and slightly higher during the LMM (Fig. 4A). Interannual variability is as pronounced as for coral $\delta^{18}O$.

The linear trend towards isotopic depletion in the late 20th century, as observed in other coral records from different ocean basins, is weak in our coral record. This might be related to growth close to the sea-surface where incoming solar radiation and surface ocean evaporation are highest. This might lead to slightly heavier isotopic values of the surface water (upper 1 m), a signal that is incorporated into the coral skeleton. The annual growth rate, however, is not diminished in the late 20th century and is only weakly correlated with coral $\delta^{18}O$ (r^2=0.09). Over the full record, annual growth rate and annual mean coral $\delta^{18}O$ are also not correlated. Mean annual coral growth generally ranges between 8 and 12 mm/year and is lowest during the Late Maunder Minimum (1675–1710) with 8–10 mm/year (Fig. 4C). There is also no correlation between annual growth and coral $\delta^{18}O$ during the Late Maunder Minimum (r^2=0.08) and coral $\delta^{18}O$ does not correlate with $\delta^{13}C$ (r^2=0.05) (S2). We investigated the effect of coral $\delta^{18}O$ and Sr/Ca ratios when the growth axis is off-vertical (>25°) by analyzing multiple transects overlapping by many years for the core section spanning the LMM. In general, the growth axis is nearly vertical (10–20°) throughout the LMM section, two short transects spanning the years 1690–1700 are off-vertical by >50° (Fig. 3). Only one transect (60° off-axis) shows higher isotopes and Sr/Ca ratios, so these data are excluded from the interpolation (S2). The multidecadal average (1675–1710) for coral $\delta^{18}O$ and Sr/Ca ratios for the LMM remains the highest of the entire record. We conclude that sampling artifacts due to a different angle of growth axis can be

Table 1
Regression equations for coral $\delta^{18}O$ and Sr/Ca ratios

Dataset	Resolution	Regression equation	r^2	p-value	*SE* °C	*DE* °C
$\delta^{18}O$						
Tulear in situ						
1991–1995	monthly	SST=−6.812($\delta^{18}O$)−4.807	0.85	0.0001		
1962–1965	monthly	SST=−5.254($\delta^{18}O$) +1.784	0.63	0.0001		
NCEP						
1981–1995	monthly	SST=−5.665($\delta^{18}O$)+0.635	0.81	0.0001	0.94	0.07
1981–1995	**mean annual**	**SST=−5.298($\delta^{18}O$)+2.061**	**0.82**	**0.0001**	**0.37**	**0.04**
GISST2.3b						
1981–1995	monthly	SST=−5.238($\delta^{18}O$)+2.389	0.75	0.0001	0.94	0.06
1981–1995	**mean annual**	**SST=−3.708($\delta^{18}O$)+9.191**	**0.61**	**0.0001**	**0.36**	**0.04**
1973–1995	**monthly**	**SST=−4.996($\delta^{18}O$)+3.617**	**0.76**	**0.0001**		
1871–1995	bimonthly	SST=−4.698($\delta^{18}O$)+4.567	0.65	0.0001		
Sr/Ca						
Tulear in situ						
1991–1995	monthly	Sr/Ca=10.011−0.037(SST)	0.74	0.0001		
NCEP						
1981–1995	extreme values	Sr/Ca=10.484−0.054(SST)	0.9	0.0001	1.1	0.06
GISST2.3b						
1981–1995	extreme values	Sr/Ca=10.319−0.049(SST)	0.89	0.0001	1.1	0.06
1973–1995	**mean annual**	**Sr/Ca=10.399−0.053(SST)**	**0.38**	**0.08**	**0.46**	**0.07**
1973–1995	**extreme values**	**Sr/Ca=10.348−0.05(SST)**	**0.89**	**0.0001**	**1.1**	**0.06**
1891–1910	monthly	Sr/Ca=10.323−0.05(SST)	0.61	0.0001		
1891–1909	**mean annual**	**Sr/Ca=12.035−0.117(SST)**	**0.54**	**0.0005**		

Linear, zero-lag OLS regression equations between coral $\delta^{18}O$ and coral Sr/Ca ratios and several sea-surface temperature (SST) data sets. The relevant calibrations used for SST reconstruction are indicated in bold fonts. SE=rooted mean squared error, DE=pooled decadal mean uncertainty.

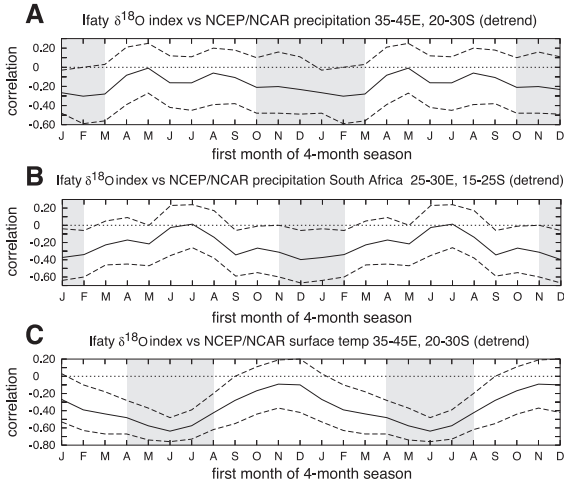

Fig. 6. Seasonal mean correlation averaged over 4-month periods between coral $\delta^{18}O$ and (A) NCEP/NCAR precipitation averaged over 35–45°E, 20–30°S [57], (B) NCEP/NCAR precipitation over South African summer rainfall region averaged over 25–30°E, 15–25°S [57], and (C) NCEP/NCAR sea-surface temperature averaged over 35–45°E, 20–30°S (http://www.cdc.noaa.gov/cdc/data.ncep.reanalysis.derived.html). Each month on the *X*-axis represents the first month of the 4-month season. The seasons with statistically significant correlation >95% are shaded. The dashed band around the correlations indicates the 95% confidence limits. Correlations computed at http://climexp.knmi.nl/.

excluded in producing heavier coral $\delta^{18}O$ and higher Sr/Ca ratios during the LMM.

4.2. Calibration of proxy data

4.2.1. Monthly and seasonal mean calibration

In order to test the reliability of coral $\delta^{18}O$ and Sr/Ca ratios to record SST variability we performed a calibration excersise for the years 1973–1995. Calibration with instrumental SST (local and gridded) was evaluated using standard ordinary least squares regression.

The annual cycle in coral $\delta^{18}O$ is very strong over the entire record and its amplitude ranges between 0.7‰ and 1.2‰. Sr/Ca ratios range between 0.19 and 0.27 mmol/mol. The seasonal amplitudes of coral $\delta^{18}O$ and Sr/Ca ratios are consistent with the average annual SST cycle varying between 4.5 and 6 °C (0.2‰ per 1 °C; 0.05 mmol/mol per 1 °C) [40,41]. Coral $\delta^{18}O$ and Sr/Ca show a high correlation (r=0.87) and record well the seasonality (Fig. 5; Table 1). Consequently, on a seasonal scale coral $\delta^{18}O$ and Sr/Ca at this location primarily reflects SST variability (Fig. 5; Table 1). However, Sr/Ca ratios display the summer SST better than the winter values (Fig. 5). The slopes of the monthly $\delta^{18}O$/SST calibrations range from 0.17‰ to 0.19‰/°C and fall well within the range of published relationships, which range from 0.18‰ to 0.22‰/°C [50–53]. The slope of the calibration between Sr/Ca ratios and instrumental SST ranges from 0.05 to 0.068 mmol/mol per 1 °C and also falls within the range of published relationships between 0.04 and 0.08 mmol/mol per 1 °C [54–56].

Occasionally, the $\delta^{18}O$ does not reflect the observed SST accurately, e.g. seasonality is slightly decreased or increased (Fig. 5). Those years are associated with lower (1978, 1983, 1985, 1987, 1990, 1992) or higher precipitation anomalies (1974–1976, 1984, 1988, 1991) during austral summer (Fig. 5) [57]. A correlation of seasonal mean rainfall anomalies derived from the NCEP/NCAR reanalysis data set (1948–1995; averaged over 35–45°E, 20–30°S; http://www.cdc.noaa.gov/cdc/data.ncep.reanalysis.derived.html) with coral $\delta^{18}O$ shows a clear relationship during austral summer (NDJF) significant above the 90% level (Fig. 6). This also holds for a correlation with South African summer rainfall averaged over 25–30°E and 15–25°S (significant >95%) (Fig. 6). Thus, summer coral $\delta^{18}O$ is also related to changes in the regional hydrologic (P–E) balance.

A spatial correlation of the mean summer (SONDJF) and winter (MJJAS) values in coral $\delta^{18}O$ and Sr/Ca ratios show a remarkable agreement with Indian Ocean SST patterns for the period 1973–1995 (Fig. 7). Correlation of coral $\delta^{18}O$ with SST is highest during winter (MJJAS; r=0.6), whereas the summer correlation (NDJF, r=0.3) is weaker. During the entire 20th century, coral $\delta^{18}O$ winter values agree very well with winter SST in the Southern Mozambique Channel and the Agulhas Current region (r=0.5). Sr/Ca displays the summer SST better than the winter pattern (Figs. 5 and 7).

4.2.2. Annual mean calibration

In addition to the monthly data, we calculated annual means for $\delta^{18}O$, Sr/Ca ratios and instrumental SST because the high autocorrelation between monthly records can bias the interpretation of the relationship between two variables [54].

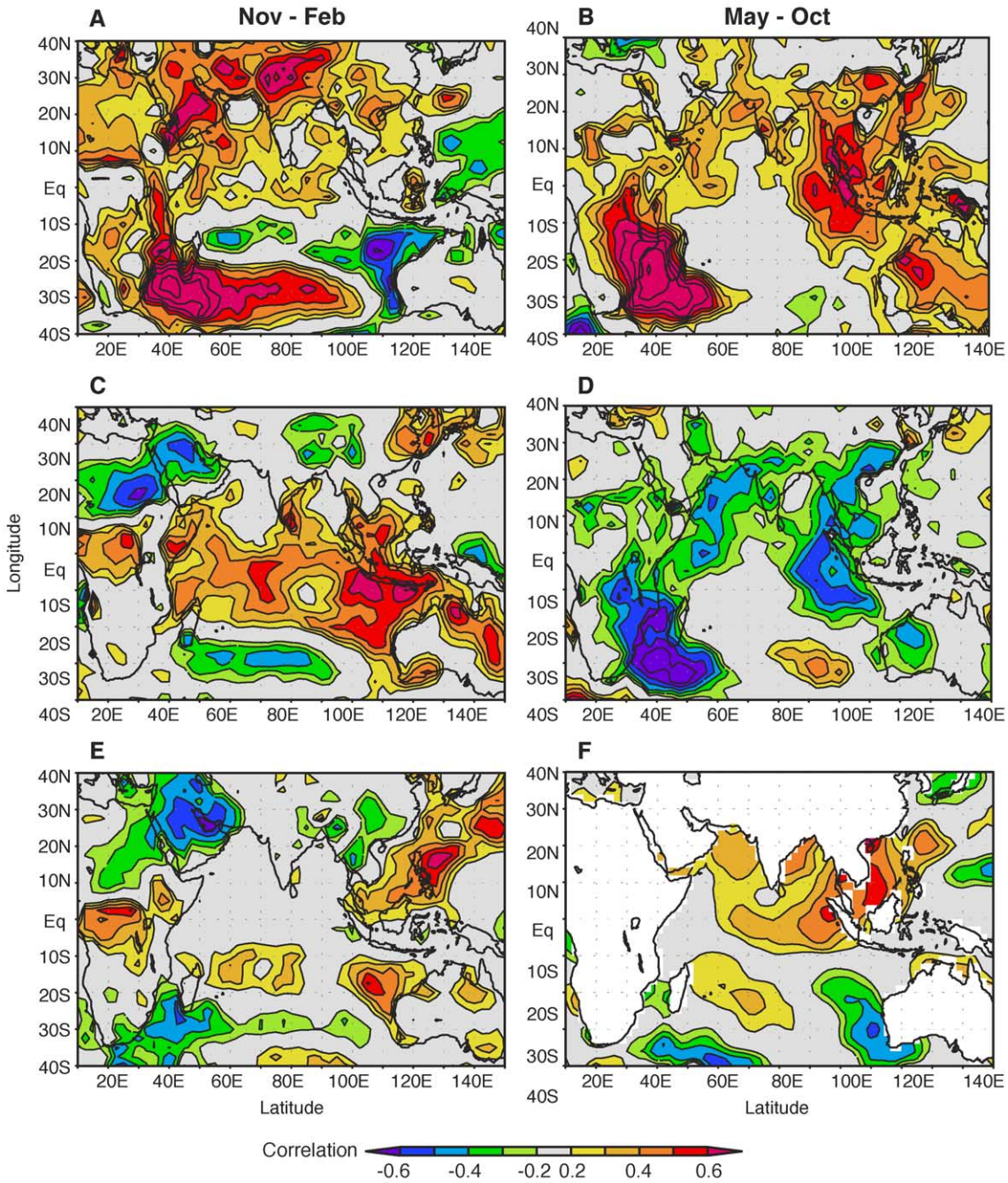

Fig. 7. Spatial correlation maps of monthly NCEP/NCAR surface temperature anomalies averaged over 40°N–40°S and 10°E–150°E over November–February (left) and May–October (right) for the period 1975–1995 (http://www.cdc.noaa.gov/cdc/data.ncep.reanalysis.derived.html) with (A and B) NCEP/NCAR surface temperature averaged over 35–45°E, 20–30°S; (C and D) monthly Ifaty-4 coral $\delta^{18}O$ anomalies (with average seasonal cycle removed) and (E and F) monthly Ifaty-4 coral Sr/Ca anomalies (with average seasonal cycle removed), all averaged over November–February (left) and May–October (right) for the period 1975–1995. The correlation coefficient is indicated in the legend. The correlations are significant above the 95% significance level. Maps created with http://climexp.knmi.nl/.

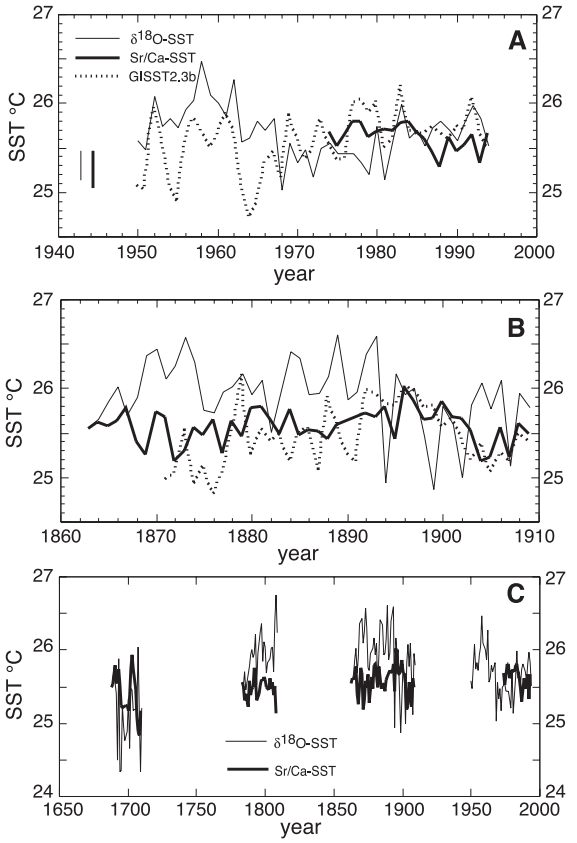

Fig. 8. Mean annual proxy-based SST variations and instrumental SST variations [47] for (A) the period 1950–1995, (B) the period 1863 to 1910 and (C) reconstructed δ^{18}O-SST and Sr/Ca-SST for all time windows with tandem measurements of coral Sr/Ca and δ^{18}O. The proxy-based annual mean SST reconstructions are based on the linear regression equations: SST=[−3.708(δ^{18}O)+9.191] (r^2=0.61) and Sr/Ca=[10.399−0.053(SST)] (r^2=0.38), respectively. Oxygen isotope derived SST (thin solid line), Sr/Ca derived SST (thick solid line) and GISST2.3b (dashed line) [47]. The rooted mean squared error for coral Sr/Ca- (0.46 °C) and δ^{18}O (0.36 °C) based SST is indicated by vertical bars.

The regression of annual means for coral δ^{18}O against SST yields a high correlation (r^2=0.76) over the calibration period from 1981 to 1995 (Table 1). The slope of the δ^{18}O/SST calibration ranges from 0.19‰ to 0.27‰/°C for NCEP and GISST2.3b, respectively [47,48]. The slope of 0.27‰/°C is too high and indicates that interannual changes in the freshwater balance probably influence the coral δ^{18}O signal. However, the 22-year average δ^{18}O-SST for the calibration period agree well with the decadal average in instrumental SST (Fig. 8A). The coral δ^{18}O reproduces successfully the general trend in annual mean SST's over most of the 20th century.

The slope of the Sr/Ca-SST relationship is 0.053 mmol/mol and is consistent with existing published literature [56]. However, the correlation is weak, albeit significant at the 99% confidence level (r^2=0.38; Table 1). The 22-year average Sr/Ca-SST record for the calibration period agree well with the multidecadal average in instrumental SST (Fig. 8A).

5. Discussion

5.1. Validation of annual mean SST reconstruction

We test the reliability of Sr/Ca ratios as an independent SST proxy by selecting the time window from 1871 to 1910 for which independent SST reconstructions are available [47–49]. Our calibration experiment shows that during the time interval from 1973 to 1995 interannual Sr/Ca ratios reflect SST changes.

During the validation period 1871–1910, interannual coral δ^{18}O is not very well correlated with GISST2.3b, whereas Sr/Ca agree well with SST reconstructions on a seasonal (r^2=0.61) and interannual time scale (r^2=0.54; Table 1; Fig. 8B). The slope of the [Sr/Ca]/SST regression is 0.053 mmol/mol per 1 °C and is well in the range of published relationships [53,61,62]. The average reconstructed Sr/Ca-SST for the entire 40-year segment of the validation period indicates 0.24 °C cooler SST compared to the calibration segment (1973–1995), consistent with the GISST2.3b estimate of a cooling by 0.26 °C (Fig. 8B). Thus, coral Sr/Ca ratios are a suitable SST indicator during the validation period and can be used to separate interannual $\delta^{18}O_{seawater}$ and SST variations further back in time.

Between 1784 and 1809 the recontructed Sr/Ca-SST indicates a cooling of about 0.26 °C compared to the present, in agreement with reconstructions of southern ocean SST [62]. The inferred warming of 0.3 °C in δ^{18}O-SST should therefore be interpreted as a response to significant $\delta^{18}O_{seawater}$ variations (Fig. 8C).

During the coldest period, the Late Maunder Minimum (1688–1710), interannual fluctuations in coral δ^{18}O and Sr/Ca agree well (Fig. 8C). Multidecadal average SST derived from the δ^{18}O and Sr/Ca

ratios indicate a significant cooling of about 0.33 or 0.47 °C compared to the present, respectively (Fig. 8C). This is in excellent agreement with a 500-year climate simulation showing only a slight cooling in the tropics and subtropics in the range of 0.3–0.5 °C during the LMM [58]. Independent regional evidence for a tropical/subtropical cooling of 0.3–0.5 °C during the Late Maunder Minimum between 1675 and 1710 comes from tree ring chronologies and speleothemes from the South African summer and winter rainfall region [59–63]. Coral records going back to 1650 from the Great Barrier Reef, New Caledonia, Galapagos and Puerto Rico also show a consistent picture of cooling during the LMM [64–68]. However, a uniform cooling during the entire Little Ice Age (1400–1850) is not observed in the tropical/subtropical coral records from the Southern Hemisphere.

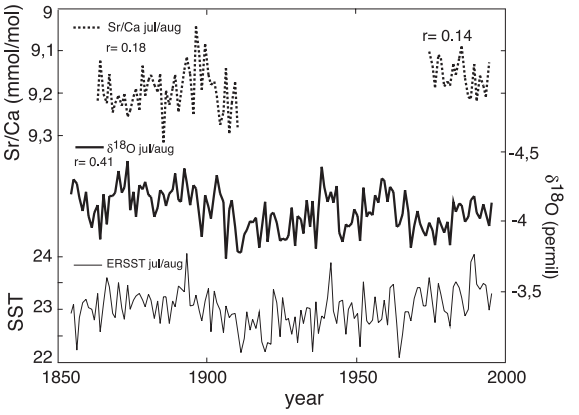

Fig. 9. Comparison of peak austral winter (July/August) Ifaty-4 coral Sr/Ca and δ^{18}O time series with ERSST v.2 for the period 1854 to 1995 [48]. Correlation coefficients with ERSST v.2 are indicated.

5.2. Mozambique Channel/Agulhas Current region austral winter SST variability over 336 years

The potential importance of the greater Agulhas Current system for the regional climate and weather patterns during the 20th century is well established [13,23,30,70–72]. It was observed that the greatest variability over the greater Agulhas Current region, including the Southern Mozambique Channel, occurs in austral winter between June and September [72]. Low SSTA in the greater Agulhas Current region are associated with a substantial decrease of heat transfer to the atmosphere, a southward shift in extratropical storm tracks, an anticyclonic anomaly over the southwestern Indian Ocean and more westerly wind anomalies [72]. A reduction in rainfall over the South African winter-rainfall-region results from these circulation anomalies due to cooler and drier air mass over the region. In contrast, warm austral winter SSTA leads to increased rainfall.

The Ifaty coral record resembles the spatial and temporal variability in austral winter SST in the greater Mozambique Channel/Agulhas Current region and adjacent South African landmass in the youngest part of the coral record from 1973 to 1995 (Fig. 7). This winter relationship is stable between 1854 and 1995 (Fig. 9). Winter coral δ^{18}O is coherent with ERSST v.2 on decadal (9–12 years) and multidecadal frequencies (S3) [48]. The better fit of winter δ^{18}O might be due to a substantially deeper mixed layer (60 m) in austral winter and therefore a more homogeneously mixed surface water column than in summer (10–20 m). Since evaporation exceeds precipitation in the annual mean during austral winter, coral δ^{18}O is less perturbed by local precipitation changes. However, changes in oceanic advection related to varying strength of the SEC may alter the δ^{18}O signal during austral winter and should be taken into account [35]. A stronger SEC related to stronger Pacific and Indian Ocean trade winds was observed for the period 1879–1899 and after 1963 to the present [16,18,25,69]. Coral δ^{18}O anomalies are negative during those periods potentially implying a contribution of warm tropical water masses by a stronger southward transport via the SEC.

In summary, the Ifaty coral record provides a measure of winter SST variability in the Mozambique Channel/Agulhas Current region on interannual and interdecadal time scales for 336 years. Positive coral δ^{18}O anomalies, indicating cool SST anomalies (SSTA), are observed between 1675–1760 (including the Late Maunder Minimum), 1810–1850, 1900–1930 and 1970–1980 (Figs. 4 and 9; S1). Negative coral δ^{18}O anomalies, indicating high winter SST, are observed between 1780–1810, 1870–1900, and 1940–1970 and 1980–1995 (Figs. 4 and 9; S1). According to the relationships established at the beginning of this chapter [72], the cooler epochs would imply a southward shift in storm tracks and

generally cooler and drier air masses over the southwestern Indian Ocean.

Future work will focus on a multi-core comparison with suitable coral records from the tropical/subtropical southeastern Indian Ocean that will potentially allow reconstruction of temporal and spatial variability in subtropical SST during austral winter and its relation to the strength of the Asian monsoon.

5.3. Austral summer coral $\delta^{18}O$ variability over 336 years

5.3.1. Deconvolving $\delta^{18}O_{seawater}$ variations: ENSO and subtropical dipole

Coral $\delta^{18}O$ is influenced by both SST and $\delta^{18}O_{seawater}$, which is related to the balance between precipitation and evaporation [1,7,8,54,73]. Downcore reconstruction of $\delta^{18}O_{seawater}$ can yield important information about past changes in hydrologic balance and oceanographic circulation [67,73].

The calibration studies established that Sr/Ca is correlated on interannual time scales with reconstructed GISST2.3b and ERSST v.2, hence we applied the approach of [73] to deconvolve the $\delta^{18}O_{seawater}$ variations. The method separates SST and seawater contributions to the coral $\delta^{18}O$ by calculating the instantaneous changes in $\delta^{18}O$ and Sr/Ca (or observed SST). By finding the contribution of SST from the reconstructed SST by using Sr/Ca (or directly from observed SST), the contribution by $\delta^{18}O_{seawater}$ can be estimated.

A negative correlation between coral $\delta^{18}O_{SST\ contribution}$ and that of $\delta^{18}O_{seawater\ contribution}$ is prevalent through the core (Fig. 10). The SST contribution clearly dominates coral $\delta^{18}O$ seasonality. In the calibration interval (1973–1995), the reconstructed $\delta^{18}O_{seawater}$ signal derived from the Ifaty coral shows seasonal variations of up to 0.7‰ for individual years which correspond to extreme wet (1974, 1976, 1984, 1991, 1993) or dry events (1978, 1983, 1985, 1992) (Fig. 10).

Dry years during austral summer over the SW Indian Ocean are associated with strong El Niños (i.e. 1972/73, 1978, 1983, 1988, 1992) and/or negative subtropical dipole events (SIOD) (i.e. 1970, 1978, 1983, 1984/85, 1992, 1995), while wet years occur during La Niñas (i.e. 1971/72, 1974, 1976, 1984) and/or positive SIOD events (1973/74, 1975/76, 1979, 1980–1982, 1993/94) (Fig. 10) [28,74]. Coincident

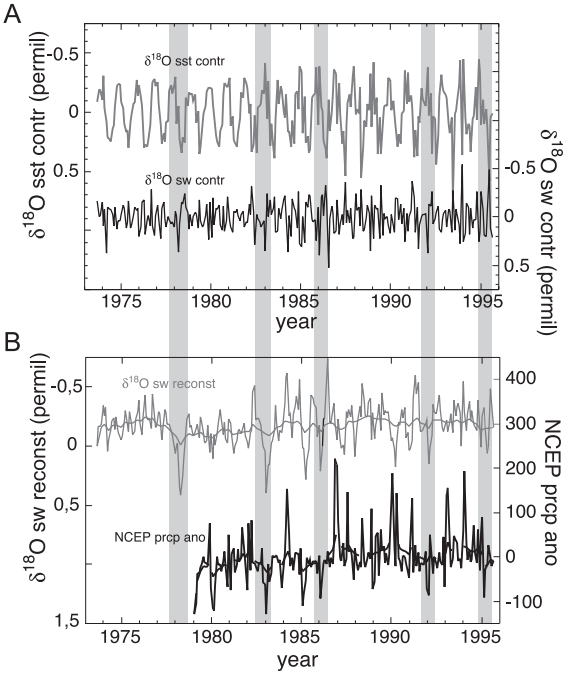

Fig. 10. Deconvolving the $\delta^{18}O_{seawater}$ component from coral $\delta^{18}O$: (A) monthly variations in coral $\delta^{18}O_{sst\ contribution}$ versus coral $\delta^{18}O_{seawater\ contribution}$ using instrumental GISST2.3b after the method in [73] and (B) coral $\delta^{18}O_{seawater\ reconstructed}$ using GISST2.3b after method in [73] versus NCEP/NCAR precipitation anomaly [57]. El Niño years (http://www.cpc.noaa.gov:80/products/analysis_monitoring/ensostuff/ensoyears.html) are indicated by shaded vertical bars.

with that pattern, coral $\delta^{18}O$ seasonality is reduced during strong El Niño (1978, 1983, 1992) or negative SIOD (1983–1985, 1992, 1995), while it is enhanced during strong La Niña (1974, 1976) or positive SIOD (1974, 1976, 1980–1982, 1991, 1993). In summary, the larger impact of ENSO on SW Indian Ocean SST and atmospheric circulation, together with different climatic boundary conditions steered by subtropical Indian Ocean dipole events, modulate the coral $\delta^{18}O$/SST relationship during austral summer.

5.3.2. ENSO teleconnections

The connection between South African summer rainfall (SARI) and ENSO and/or SIOD is well established [13,17,19,20,24,27–31]. High SST in the Mozambique Channel/Agulhas Current region usually favours more intense rainfall over the SARI-region and vice versa for low SST. However, this historical

relationship has broken down after 1970 [24]. Consequently, high southwestern Indian Ocean SSTs are associated with a persistent drought in SARI-region. This indicates that the relationship between regional SST and large-scale atmospheric circulation has changed after the 1970s. This change is most probably related to an abrupt change of the Pacific climate state, the so-called 1970s shift [26]. El Niño modifies the southern Indian Ocean Walker circulation cell with a shift of the ascending branch (deep convection area) over the SW Indian Ocean and Madagascar and the subsiding branch over southeastern Africa, which leads to a drought over the SARI region [12,24,27]. This pattern is consistent with studies showing an inverse relationship between Madagascar (MASR)- and southern Africa summer-rainfall from the early 1960s to the present [14,15] (Fig. 11). This modified east–west circulation is probably forced by a warmer southern Indian Ocean after the late 1960s [24].

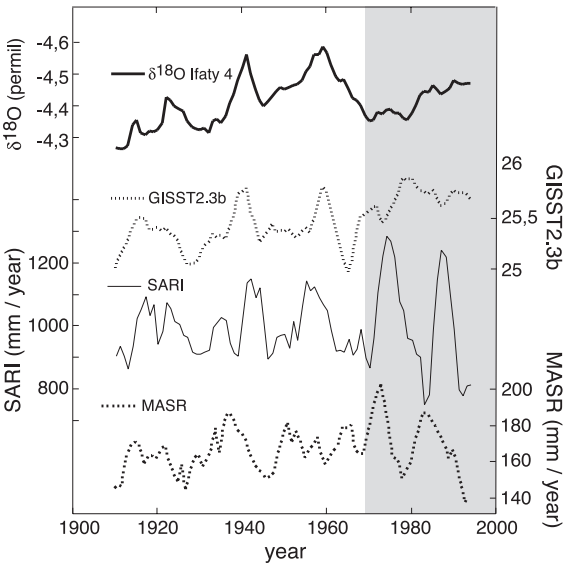

Fig. 11. Comparison between mean summer (NDJF) coral $\delta^{18}O$ (thick solid line), mean summer (NDJF) GISST2.3b (thin stippled line) [47], South African Rainfall Index (SARI; thin solid line) [17] and Madagascar Summer Rainfall (MASR) averaged over 30–50°E, 15–25°S [57]. The values are computed as a 9-point moving average. The recent period between 1970 and 2000 is indicated by gray shading to highlight the anticorrelation between South Africa summer rainfall Index (SARI) and Madagascar summer rainfall Index (MASR).

In order to analyze the connection between the austral summer coral $\delta^{18}O$ and the ENSO phenomenon, we performed statistical analysis for the period 1856 to 1995. The MTM spectrum of coral $\delta^{18}O$ shows a prominent interannual frequency of 2.2 and 3.9 years significant above the 99% level (S4). A wavelet cross spectrum shows evidence that interannual variability within the 2–4-year frequency band in coral $\delta^{18}O$ (JF) and NINO3 Index (JF) is coherent and in phase (phase 0–30°) (Fig. 12A). This relationship strongly suggests that the 2–4-year period in our coral record is related to ENSO. Therefore, we calculated coral $\delta^{18}O$ and gridded Kaplan-SST and SLP [49,75] for January/February and the entire austral summer (SONDJF) for comparison with ENSO indices (NINO3 Index [49], SOI index [74]), because maximum correlation is found for these month.

A 20-year moving correlation between Kaplan-SLP (SONDJF) at the coral site and NINO3 Index (SONDJF) shows a high correlation between the records (Fig. 12B). Highest correlations are indicated between 1860–1930 and 1960–1995, whereas it is weaker between 1930 and 1960. A field correlation of SST at the coral site (SONDJF) versus global SST [48] separated into the epochs 1950–1975 and 1976–1995 indicates that ENSO correlation is higher and spatially consistent in the latter epoch (S5). This is in good agreement with other studies in showing a large influence of ENSO on SW-Indian Ocean SST and rainfall variability between 1960 and the present and weaker before [24,27]. Coherent and robust spatial correlation structures in Indian Ocean SST, SLP and circulation patterns with ENSO were also established between 1880 and 1920 [16]. This is supported by a high correlation between regional sea-level pressure at the coral site with ENSO Indices during austral summer (SONDJF) between 1860–1920 and after the 1960s (Fig. 9B) [24].

The coral $\delta^{18}O$ record successfully captures the ENSO teleconnection as shown by a running correlation between coral $\delta^{18}O$ (SONDJF) and NINO3 Index (SONDJF) (or SOI-Index). High correlation coefficients are indicated between 1870–1930 and after 1960–1990 (Fig. 12B). Higher coral $\delta^{18}O$ (SONDJF) are associated with higher SST in the NINO3 region during an El Niño between 1890–1930 and 1960–1990 and vice versa for La Niña. A field correlation map of coral $\delta^{18}O$ (SONDJF) versus global SST [49] separated into the epochs 1950–1975 and 1976–1995 indicates that ENSO correlation is higher and spatially

consistent in the latter epoch, in agreement with regional SST correlation patterns (S5). Coral $\delta^{18}O$ (SONDJF) also shows a close relationship with the SARI prior to 1970, which weakened thereafter, consistent with the regional SST/SARI relationship in response to ENSO (Fig. 11). This indicates that the austral summer coral $\delta^{18}O$ between 1856 and 1995 reflects changes in the hydrologic balance in the

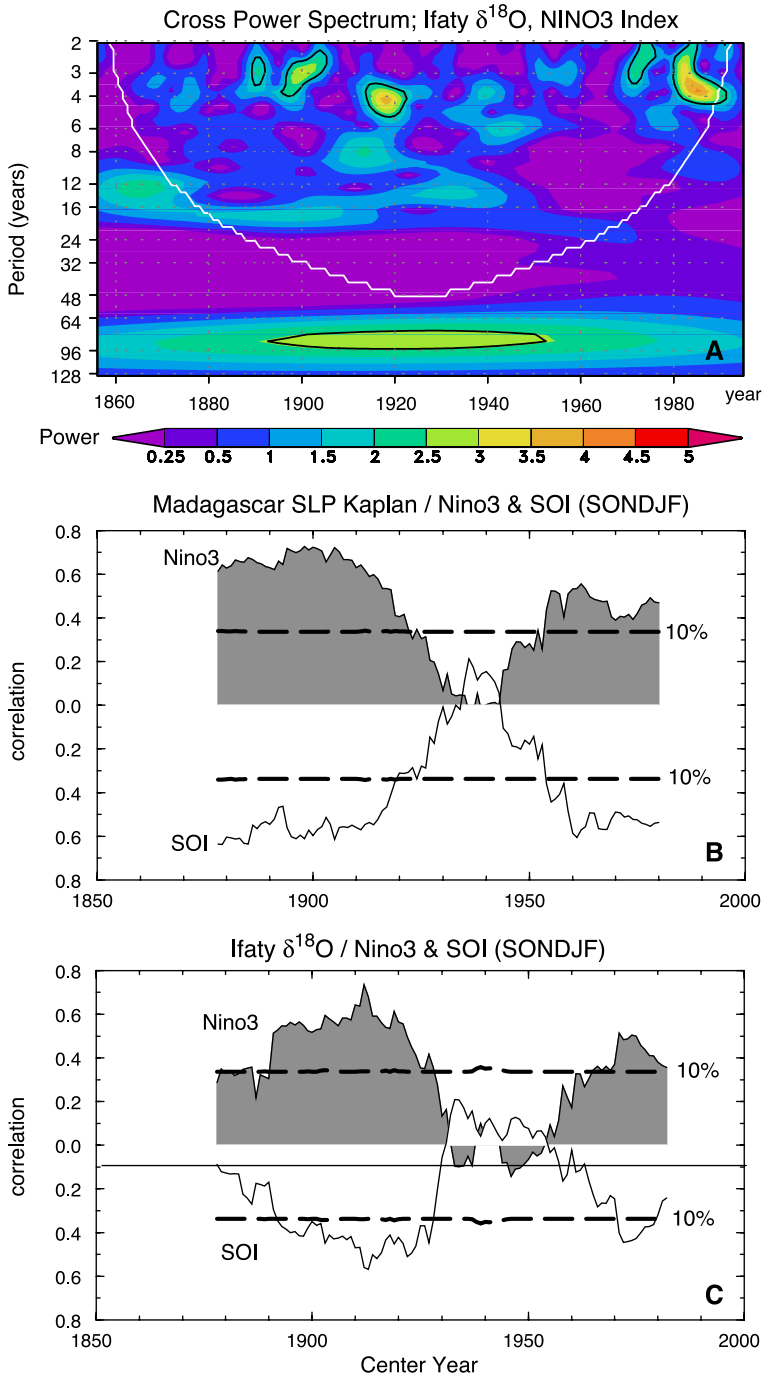

southern Mozambique Channel that are related to ENSO. Consequently, we can examine the coral δ^{18}O/ ENSO relationship for the entire record.

All in all, interannual variability in the ENSO frequency band in austral summer coral δ^{18}O record over the last 336 years is strongest in amplitude between 1680–1720, 1760–1790, 1870–1920, 1930–40 and 1960–1995 (S6). Comparison with other oceanic proxy reconstructions for the period before 1856 is limited. However, high amplitude ENSO variability in the Ifaty coral coincides with more frequent and intense El Niño events documented in the Palmyra coral record from the tropical Pacific for the 17th century [76]. The Galapagos coral δ^{18}O shows highest amplitude variations in the interannual ENSO band between 1645–1715 and the late 18th century, again consistent with the Ifaty record [2]. The Ifaty coral agrees with the reconstructed Nino3 Index in showing high amplitude ENSO variability in the early and late 18th century [77].

6. Conclusions

The 336-year Ifaty coral oxygen isotope record off southwestern Madagascar reflects changes in SST on seasonal to multidecadal time scales. The coolest period is recorded between 1675 and 1760 and it includes the Late Maunder Minimum (1675–1710). The warmest periods occur between 1880–1900 and the period 1973–1995. This conclusion is ground-truthed by Sr/Ca measurements as an independent SST indicator for selected time windows. We show evidence that the Ifaty record mirrors the spatial and temporal variability in austral winter SST in the greater Mozambique Channel/Agulhas Current region and adjacent South African landmass back to 1854. Austral summer coral oxygen isotopes are influenced by changes in the hydrological balance (evaporation–precipitation). Variations in the hydrologic balance in the early and late 20th century appear to be related to large scale atmospheric circulation anomalies originating in the Pacific, i.e. ENSO, and in subtropical Indian Ocean dipole events. The Ifaty δ^{18}O and Sr/Ca record shows that the impact of ENSO on SW Indian Ocean SST and atmospheric circulation was strong between 1680–1720, 1760–1790, 1870–1920, 1930–1940 and after 1970. The Ifaty coral record demonstrates that the SW Indian Ocean SST has changed considerably during the last 300 years. This changing "base-state" seems to alter the spatial signature of ENSO thereby effecting the relationship between local SST and evaporation/precipitation balance in the Mozambique Channel. This conclusion is supported by a nonstationary correlation of our coral record with the NINO3 Index.

The Ifaty coral record provides a proxy time series for SST variability and hydrological changes in the greater Agulhas Current region that can be potentially used, in conjunction with suitable eastern Indian Ocean corals, to reconstruct spatial and temporal variability in the Indian Ocean subtropical dipole and its relation to the Indian monsoon.

Acknowledgments

We would like to thank the TESTREEF-group for the drilling of the coral core within the lagoon of Ifaty in 1995, especially B.A. Thomassin (COM, Marseille) and Marco Taviani (University Bologna). We thank B.A. Thomassin (COM, Marseille) for helpful comments on environmental parameters in the lagoons of Ifaty and Tulear. We thank A. Kolevica for assistance in Sr/Ca sample preparation. M. Joachimski (University Erlangen) carried out the isotope measurements. B. Schnetger (ICBM University Oldenburg) supervised ICP-AES measurement. Comments on an early version of this manuscript

Fig. 12. (A) Cross Wavelet Spectrum between mean summer (SONDJF) coral δ^{18}O and NINO3 Index [49] for the period 1856 to 1995. Black contours indicate that the amplitude within is significant at the 95% level against a red noise background. Stippled line delineates the cone of influence, where zero padding has reduced the variance. (B) Running correlations between the mean summer (SONDJF) sea level pressure anomalies at the coral site [76] and mean summer (SONDJF) NINO3 index [49] and mean summer (SONDJF) Southern Oscillation Index (white area) [74], respectively. (C) Running correlations between the mean summer (SONDJF) coral δ^{18}O and mean summer (SONDJF) NINO3 index (gray shaded area) and mean summer (SONDJF) Southern Oscillation Index (white area). Correlations are computed with 21-year sliding windows. Dashed lines indicate 10% significance levels (two-tailed test) taking into account the autocorrelation of the time series. Running correlations are plotted at the center of each 21-year period. (For colours see the online version of this article.)

from M. Pfeiffer (IFM-GEOMAR, Kiel), G.R. Davies, F. Peeters, G. Ganssen and D. Kroon (all Vrije Universiteit, Amsterdam) were invaluable. The authors would like to acknowledge O. Tim (IFM-GEOMAR, Kiel) for computing assistance and help in statistics. This research was supported by the German government through the KIHZ-Initiative. Comments of two anonymous reviewers helped improve the clarity of the manuscript.

Appendix A. Supplementary data

Supplementary data associated with this article can be found, in the online version, at doi:10.1016/j.epsl.2004.09.028.

References

[1] J.E. Cole, R.G. Fairbanks, G.T. Shen, Recent variability in the Southern Oscillation: isotopic results from a Tawara Atoll record, Science 260 (1993) 1790–1793.
[2] R.B. Dunbar, G.M. Wellington, M.W. Colgan, P.W. Glynn, Eastern Pacific sea surface temperatures since 1600 A.D.: the delta18O record of climate variability in Galàpagos corals, Paleoceanography 9 (2) (1994) 291–315.
[3] M.T. McCulloch, M.K. Gagan, G.E. Mortimer, A.R. Chivas, P.J. Isdale, A high-resolution Sr/Ca and delta 18O coral record from the Great Barrier Reef, Australia, and the 1982–1983 El Nino, Geochim. Cosmochim. Acta 58 (12) (1994) 2747–2754.
[4] C.D. Charles, D.E. Hunter, R.G. Fairbanks, Interaction between the ENSO and the Asian Monsoon in a coral record of tropical climate, Science 277 (1997) 925–928.
[5] T.M. Quinn, T.J. Crowley, F.W. Taylor, C. Henin, P. Joannot, Y. Join, A multicentury isotopic record from a New Caledonia coral: Interannual and decadal sea surface temperature variability in the southwest Pacific since 1657 AD, Paleoceanography 13 (4) (1998) 412–426.
[6] H. Kuhnert, J. Pätzold, B. Hatcher, K.-H. Wyrwoll, A. Eisenhauer, L.B. Collins, Z.R. Zhu, G. Wefer, A 200-year coral stable oxygen isotope record from a high-latitude reef off Western Australia, Coral Reefs 18 (1999) 1–12.
[7] N. Le Bec, A. Juillet-Leclerc, T. Corrège, D. Blamart, T. Delcroix, A coral d18O record of ENSO driven sea surface salinity variability in Fiji (south-western tropical Pacific), Geophys. Res. Lett. 27 (23) (2000) 3897–3900.
[8] E.J. Hendy, M.K. Gagan, C.A. Alibert, M.T. McCulloch, J.M. Lough, P.J. Isdale, Abrupt decrease in tropical Pacific sea surface salinity at end of Little Ice age, Science 295 (2002) 1511–1514.
[9] R.S. Bradley, P.D. Jones, Climate Since A.D. 1500, Routledge, London, 1993, 665 pp.
[10] J. Lutterbacher, R. Rickly, E. Xoplaki, C. Tinguely, C. Beck, C. Pfister, H. Wanner, The Late Maunder Minimum (1675–1715): a key period for studying decadal scale climatic change in Europe, Climate Change 49 (2001) 441–462.
[11] E. Zorita, H.v. Storch, F.J. Gonzales-Rouco, U. Cubasch, J. Lutterbacher, S. Legutke, I. Fischer-Bruns, U. Schlese, Simulation of the climate of the last five centuries, GKSS-Report 12 (2003) (43 pp.).
[12] P.D. Tyson, Climate change and variability in Southern Africa, Oxford University Press, Cape Town, 1986, 217 pp.
[13] N.D. Walker, Links between South African summer rainfall and temperature variability of the Agulhas and Benguela current system, J. Geophys. Res. 95 (C3) (1990) 3297–3319.
[14] M.R. Jury, B. Pathack, A study of climate and weather variability over the tropical southwest Indian Ocean, Meteorol. Atmospher. Phys. 47 (1991) 37–48.
[15] M.R. Jury, B.A. Parker, N. Raholijao, A. Nassor, Variability of summer rainfall over Madagascar: climate determinants at interannual scales, Int. J. Climatol. 15 (1995) 1323–1332.
[16] R.J. Allan, J.A. Lindesay, C.J.C. Reason, Multidecadal variability in the climate system over the Indian Ocean region during the austral summer, J. Climate 8 (1995) 1853–1873.
[17] S.J. Mason, Sea-surface temperature–south African rainfall associations, 1910–1989, Int. J. Climatol. 15 (1995) 119–135.
[18] C.J.C. Reason, R.J. Allan, J.A. Lindesay, Evidence for the influence of remote forcing on interdecadal variability in the southern Indian Ocean, J. Geophys. Res. 101 (C5) (1996) 11876–11882.
[19] C.J.C. Reason, C.R. Godfred-Spenning, R.J. Allan, J.A. Lindesay, Air–sea interaction mechanisms and low-frequency climate variability in the south Indian Ocean region, Int. J. Climatol. 18 (1998) 391–405.
[20] S.E. Nicholson, J. Kim, The relationship of the El Nino–Southern Oscillation to African rainfall, Int. J. Climatol. 17 (1997) 117–135.
[21] A. Rocha, I. Simmonds, Interannual variability of south-eastern African summer rainfall: Part II. Modelling the impact of sea-surface temperature on rainfall and circulation, Int. J. Climatol. 17 (1997) 267–290.
[22] S. Power, T. Casey, C. Folland, A. Colman, V. Mehta, Interdecadal modulation of the impact of ENSO on Australia, Climate Dynamics 15 (1999) 319–324.
[23] C.J.C. Reason, H. Mulenga, Relationships between South African rainfall and SST anomalies in the southwest Indian Ocean, Int. J. Climatol. 19 (1999) 1651–1673.
[24] Y. Richard, S. Trzaska, P. Roucou, M. Rouault, Modification of the southern African rainfall variability/ENSO relationship since the late 1960's, Climate Dynamics 16 (2000) 883–895.
[25] R. Murtugudde, A.J. Busalacchi, J. Beauchamp, Seasonal-to-interannual effects of the Indonesian throughflow on the tropical Indo-Pacific basin, J. Geophys. Res. 103 (C10) (1998) 21.425–21.441.
[26] Y. Zhang, J.M. Wallace, D.S. Battisti, ENSO-like interdecadal variability: 1900–93, J. Climate 10 (1996) 1004–1020.
[27] C.J.C. Reason, M. Rouault, ENSO-like decadal variability and South African rainfall, Geophys. Res. Lett. 29 (2002) 10.1029.

[28] S.K. Behera, T. Yamagata, Subtropical SST dipole events in the southern Indian Ocean, Geophys. Res. Lett. 28 (2) (2001) 327–330.
[29] C.J.C. Reason, Subtropical Indian Ocean SST dipole events and southern African rainfall, Geophys. Res. Lett. 28 (11) (2001) 2225–2227.
[30] C.J.C. Reason, Sensitivity of the southern African circulation to dipole sea-surface temparature patterns in the south Indian Ocean, Int. J. Climatol. 22 (2002) 377–393.
[31] P. Terray, P. Delecluse, S. Labattu, L. Terray, Sea surface temperature associations with the late Indian summer monsoon, Climate Dynamics 21 (2003) 593–618.
[32] F.A. Schott, J.P. McCreary, The monsoon circulation of the Indian Ocean, Progress in Oceanography 51 (2001) 1–123.
[33] J.-R. Donguy, B. Piton, The Mozambique channel revisited, Oceanol. Acta 14 (6) (1991) 549–558.
[34] J.R.E. Lutjeharms, P.M. Wedepohl, J.M. Meeuwis, On the surface drift of the East Madagascar and Mozambique Currents, S. Afr. J. Sci. 96 (2000) 141–147.
[35] S.F. DiMarco, P. Chapman, W.D. Nowlin Jr., P. Hacker, K. Donohue, M. Luther, G.C. Johnson, J. Toole, Volume transport and property distributions of the Mozambique Channel, Deep-Sea Research II. Topical Studies in Oceanography 49 (2002) 1481–1511.
[36] W.P.M. De Ruijter, H. Ridderinkhof, J.R.E. Lutjeharms, M.W. Schouten, C. Veth, Observations of the flow in the Mozambique Channel, Geophys. Res. Lett. 29 (10) (2002) 140–142.
[37] M.W. Schouten, W.P.M. De Ruijter, P.J. Van Leeuwen, H.A. Dijkstra, An oceanic teleconnection between the equatorial and southern Indian Ocean, Geophys. Res. Lett. 29 (16) (2002) 59–62.
[38] A.C. Hirst, J.S. Goodfrey, The response to a sudden change in Indonesian throughflow in a global ocean GCM, J. Phys. Oceanogr. 23 (1994) 1895–1910.
[39] J.T. Potemra, Contribution of equatorial Pacific winds to southern tropical Indian Ocean Rossby waves, J. Geophys. Res. 106 (C2) (2001) 2407–2422.
[40] S. Levitus, T.P. Boyer, World Ocean Atlas 1994, U.S. Department of Commerce, Washington, DC, 1994, 99 pp.
[41] R.W. Reynolds, T.M. Smith, A high-resolution global sea surface temperature climatology, J. Climate 8 (1994) 1571–1583.
[42] J.E.N. Veron, M. Pichon, Scleractinia of eastern Australia: Part IV. Poritidae, Austral. Inst. Mar. Sci. Bull. 4 (1982) 1–159.
[43] D.W. Knutson, R.W. Buddemeier, S.V. Smith, Coral chronometers: seasonal growth bands in reef corals, Science 177 (1972) 270–272.
[44] J.H. Hudson, E.A. Shinn, R.B. Halley, B. Lidz, Sclerochronology: a tool for interpreting past environments, Geology 4 (1976) 361–364.
[45] D. Schrag, Rapid analysis of high-precision Sr/Ca ratios in corals and other marine carbonates, Paleoceanography 14 (2) (1999) 97–102.
[46] D. Paillard, L. Labeyrie, P. Yiou, Macintosh program performs time-series analysis, Eos Trans. AGU 77 (1996) 379.
[47] N.A. Rayner, E.B. Horton, D.E. Parker, C.K. Folland, R.B. Hackett, Version 2.2 of the global sea-ice and sea surface temperature dataset. Climate Research Technical Note, Hadley Centre for Climate Prediction and Research 74 (1996) 1–21.
[48] T.M. Smith, R.W. Reynolds, Improved Extended Reconstruction of SST (1854–1997), J. Climate 17 (12) (2004) 2466–2477.
[49] A. Kaplan, M.A. Cane, Y. Kushnir, A.C. Clement, M.B. Blumenthal, B. Rajagopalan, Analysis of global sea surface temperatures 1856–1991, J. Geophys. Res. 103 (C9) (1998) 18567–18589.
[50] J.N. Weber, P.M.J. Woodhead, Temperature dependance of oxygen-18 concentration in reef coral carbonates, J. Geophys. Res. 77 (3) (1972) 463–473.
[51] M.K. Gagan, A.R. Chivas, P.J. Isdale, High-resolution isotopic records from corals using ocean temperature and mass-spawning chronometers, Earth Planet. Sci. Lett. 121 (1994) 549–558.
[52] G.M. Wellington, R.B. Dunbar, G. Merlen, Calibration of stable oxygen isotope signatures in Galàpagos corals, Paleoceanography 11 (4) (1996) 467–480.
[53] A. Juillet-Leclerc, G. Schmidt, A calibration of the oxygen isotope paleothermometer of coral aragonite from *Porites*, Geophys. Res. Lett. 28 (21) (2001) 4135–4138.
[54] T.M. Quinn, D.E. Sampson, A multiproxy approach to reconstructing sea surface conditions using coral skeleton geochemistry, Palaeoceanography 17 (4) (2002) 1062.
[55] C. Alibert, M.T. McCulloch, Strontium/calcium ratios in modern Porites corals from the Great Barrier Reef as a proxy for sea surface temperature: calibration of the thermometer and monitoring of ENSO, Paleoceanography 12 (3) (1997) 345–363.
[56] J.F. Marshall, M.T. McCulloch, An assessment of the Sr/Ca ratio in shallow water hermatypic corals as a proxy for sea surface temperature, Geochim. Cosmochim. Acta 66 (18) (2002) 3263–3280.
[57] P. Xie, P. Arkin, Analysis o global monthly precipitation using gauge observations, satellite estimates, an numerical model predictions, J. Climate 9 (1996) 840–885.
[58] KIHZ-Consortium, J. Zinke, H. von Storch, B. Mueller, E. Zorita, B. Rein, B. Mieding, H. Miller, A. Luecke, G.H. Schleser, M. Schwab, J.F.W. Negendank, U. Kienerl, J.-F. Gonzalez-Rouco, W.-Chr. Dullo, A. Eisenhauer, Evidence for the climate during the Late Maunder Minimum from proxy data and model simulations available within KIHZ, in: H. von Storch, E. Raschke, G. Floeser (Eds.), The Climate in Historical Times—Towards a Synthesis of Holocene Proxy Data and Climate Models, Springer Verlag, Berlin, 2004, pp. 397–414.
[59] M.J. Hall, Dendroclimatology, rainfall and human adaption in the later Iron Age of Natal and Zululand, Annals of the Natal Museum 22 (1976) 693–703.
[60] P.W. Dunwiddie, V. LaMarche, A climatologically-responsive tree-ring record from Widdringtonia cedarbergensis, Cape Province, South Africa, Nature 286 (1980) 796–797.
[61] A.S. Talma, J.C. Vogel, Late Quaternary paleotemperatures derived from a speleothem from Cango Caves, Cape Province, South Africa, Quat. Res. 37 (1992) 203–213.

[62] P.D. Tyson, G.R.J. Cooper, T.S. McCarthy, Millennial to multi-decadal variability in the climate of Southern Africa, Int. J. Climatol. 22 (2002) 1105–1117.
[63] K. Holmgren, P.D. Tyson, A. Moberg, O. Svanered, A preliminary 3000-year regional temperature reconstruction for South Africa, S. Afr. J. Sci. 97 (2001) 49–51.
[64] E.R.M. Druffel, S. Griffin, Large variations of surface ocean radiocarbon: evidence of circulation changes in the southwestern Pacific, J. Geophys. Res. 98 (C11) (1993) 20249–20259.
[65] T. Corrège, T. Quinn, T. Delcroix, F. Le Cornec, J. Récy, G. Cabioch, Little Ice age sea surface temperature variability in the southwest tropical Pacific, Geophys. Res. Lett. 28 (18) (2001) 3477–3480.
[66] A. Winter, H. Ishioroshi, T. Watanabe, T. Oba, J. Christy, Caribbean sea surface temperatures: two-to-three degrees cooler than present during the Little Ice Age, Geophys. Res. Lett. 27 (20) (2000) 3365–3368.
[67] T. Watanabe, A. Winter, T. Oba, Seasonal changes in sea surface temperature and salinity during the Little Ice Age in the Caribbean Sea deduced from Mg/Ca and 18O/16O ratios in corals, Mar. Geol. 173 (2001) 21–35.
[68] J. Zinke, W.-C. Dullo, A. Eisenhauer, Late Maunder Minimum sea surface temperature variability recorded in corals, AGU Spring Meeting. EOS, Trans. Amer. Geophys. Union, 2002, pp. S31–S32.
[69] C.J.C. Reason, Multidecadal climate variability in the subtropics/mid-latitudes of the Southern Hemisphere oceans, Tellus 52A (2000) 203–223.
[70] M. Todd, R. Washington, Circulation anomalies associated with tropical–temperate troughs in southern Africa and the south west Indian Ocean, Climate Dynamics 15 (1999) 937–951.
[71] R. Washington, M. Todd, Tropical–temperate links in Southern African and southwest Indian Ocean satellite-derived daily rainfall, Int. J. Climatol. 19 (1999) 1601–1616.
[72] C.J.C. Reason, Evidence for the influence of the Agulhas current on regional atmospheric circulation patterns, J. Climate 14 (2001) 2769–2778.
[73] L. Ren, B.K. Linsley, G.M. Wellington, D.P. Schrag, O. Hoegh-Guldberg, Deconvolving the d18O seawater component from subseasonal coral d18O and Sr/Ca at Rarotonga in the southwestern subtropical Pacific for the period 1726 to 1997, Geochim. Cosmochim. Acta 67 (9) (2002) 1609–1621.
[74] R.J. Allan, N. Nicholls, P.D. Jones, I.J. Butterworth, A further extension of the Tahiti-S.O.I. Darwin, early SOI results and Darwin pressure, J. Climate 4 (1991) 743–749.
[75] G.A. Brook, M.A. Rafter, L.B. Railsback, S.-W. Sheen, J. Lundberg, A high-resolution proxy record of rainfall and ENSO since AD 1550 from layering in stalagmites from Anjohibe Cave, Madagascar, Holocene 9 (1) (1999) 695–705.
[76] A. Kaplan, Y. Kushnir, M.A. Cane, Reduced space optimal interpolation of historical marine sea level pressure: 1854–1992, J. Climate 13 (2000) 2987–3002.
[77] D.J. Thomson, Spectrum estimation and harmonic analysis, Proceeding IEEE 70 (1982) 1055–1096.
[78] R. Vautard, M. Ghil, Singular spectrum analysis in nonlinear dynamics, with applications to paleoclimatic time series, Physica D 35 (1989) 395–424.
[79] R. Vautard, P. Yiou, M. Ghil, Singular spectrum analysis: a toolkit for short, noisy chaotic signals, Physica D 58 (1992) 95–126.
[80] C. Torrence, G.P. Compo, A practical guide to wavelet analysis, Bull. Am. Meteorol. Soc. 79 (1) (1998) 61–78.